Journal of Thermal Analysis and Calorimetry, Vol. 65 (2001) 241–248

THERMAL DECOMPOSITION OF (4,4'-DIMETHYL-2,2'-BIPYRIDINE) TRIS(BENZOATE) EUROPIUM(III) Non-isothermal kinetics

J. J. Zhang[1*], *R. F. Wang*[2], *J. B. Li*[1] *and H. M. Liu*[3]

[1]Experimental Center, Hebei Teachers' University, Shijiazhuang, 050016 P.R. China
[2]Department of Chemistry, Hebei Teachers' University, Shijiazhuang, 050016 P.R. China
[3]Department of Chemistry and Pharmacy Engineering, Hebei University of Science and Technology, Shijiazhuang, 050018 P.R. China

(Received June 27, 2000; in revised form March 15, 2001)

Abstract

The thermal behavior of $[Eu_2(BA)_6(dmbpy)_2]$ (*BA*=$C_7H_5O_2^-$, benzoate; *dmbpy*=$C_{12}H_{12}N_2$, 4,4'-dimethyl-2,2'-bipyridine) and its kinetics were studied under the non-isothermal condition in a static air atmosphere by TG-DTG, IR and SEM methods. Thermal decomposition of $[Eu_2(BA)_6(dmbpy)_2]$ occurred in four consecutive stages at T_P 232, 360, 455 and 495°C. The kinetic parameters were obtained from analysis of the TG-DTG curves by Achar and Madhusudanan–Krishnan–Ninan (MKN) methods. The most probable mechanisms for the first stage was suggested by comparing the kinetics parameters.

Keywords: benzoic acid, europium complex, non-isothermal kinetics, thermal decomposition

Introduction

Because of the variation of coordination modes for carboxylate anions, several types of crystal structures and interesting fluorescence properties for europium carboxylate complexes were obtained [1–2]. Their thermal decomposition behavior have been reported in previous paper [3–4]. Preparation and determination of the crystal structure and luminescence spectrum of the (4,4'-dimethyl-2,2'-bipyridine) tris(benzoate) europium(III) where published earlier [5]. In this paper we discussed its thermal decomposition procedure studied by TG-DTG, IR and SEM techniques and the corresponding non-isothermal kinetics by means of the Achar method [6] and the MKN method [7], respectively.

* Author for correspondence: E-mail: jjzhang123@263.net

1418–2874/2001/ $ 5.00

Akadémiai Kiadó, Budapest
Kluwer Academic Publishers, Dordrecht

Experimental

Sample

The (4,4'-dimethyl-2,2'-bipyridine) tris(benzoate) europium(III) was prepared as described previously [5].

TG and DTG analysis

The TG and DTG curves were obtained using a Perkin Elmer TGA7 thermogravimetric analyzer. Experimental conditions were as follows: heating rate used 5°C min^{-1}; temperature range from ambient to 725°C; sample size 2.0 mg; in static air atmosphere.

Electron microscopic observations

Small quantity of the sample was dispersed on the sample holder spray Au was sprayed with Hitachi IB-5, observation was made by Hitachi S-570 scanning electron microscopy.

Infrared spectroscopic analysis

IR spectra were obtained with a Bio-Rad FTS-135 spectrometer in the range of 4000–400 cm^{-1}, using KBr pellets.

Calculation of kinetic parameters

Both Achar and MKN methods have been used to study the kinetics of the first decomposition processes of (4,4'-dimethyl-2,2'-bipyridine) tris(benzoate) europium(III). The differential and integral equations are as follows:

$$\ln\left[\frac{\frac{d\alpha}{dt}}{f(\alpha)}\right]=\ln A-\frac{E}{RT} \qquad \frac{d\alpha}{dt}=\frac{\beta d\alpha}{dT} \tag{1}$$

$$\ln\left[\frac{g(\alpha)}{T^{1.9215}}\right]=\ln\frac{AE}{\beta R}+3.7721-1.9215\ln E-0.12039\frac{E}{T} \tag{2}$$

where α is the conversion, $d\alpha/dt$ is the rate of conversion, T is the absolute temperature, A is the pre-exponential factor, R is the gas constant, E is the apparent activation energy, β is the linear heating rate, $f(\alpha)$ and $g(\alpha)$ are the differential and integral mechanism functions, respectively.

All the computational work was done on an IBM computer using a BASIC program.

Results and discussion

Thermogravimetric decomposition, IR spectra and SEM pictures

TG and DTG curves of (4,4'-dimethyl-2,2'-bipyridine) tris(benzoate) europium(III) are shown in Fig. 1. The peak temperatures and temperature range of DTG curve and the percentages of mass loss and probable composition of the leaving groups are given in Table 1. The IR spectra of some intermediate products of the thermal decomposition are shown in Fig. 2. The IR spectra of these products are completely different from that of the original complex at room temperature.

Table 1 Thermal decomposition data for $[Eu_2(BA)_6(dmbpy)_2]$ in static air atmosphere

Stage	Temp. range/°C	DTG peak temp./°C	Loss of mass/%		Prob able composition of expelled groups	Intermediate
			obs.	theory		
I	164–267	232	27.8	26.3	$-2C_{12}H_{12}N_2$	$[Eu_2(BA)_6]$
II	267–387	360	11.2	11.0	$-2C_6H_5$	$Eu_2(BA)_4(COO)_2$
III	387–479	455	17.8	17.3	–2BA	$Eu_2(BA)_2(COO)_2$
IV	479–578	495	19.3 76.1[a]	20.1 74.8[a]	$C_{16}H_{10}O_5$	Eu_2O_3

[a]Total mass loss/%

The thermal decomposition process of $[Eu_2(BA)_6(dmbpy)_2]$ can be divided into four stages. In the first stage, between 164 and 267°C, a mass loss of 27.81% is observed corresponding to the loss of the 2 mol $C_{12}H_{12}N_2$ (theoretical mass loss is 26.50%) and to the formation of $Eu_2(BA)_6$ from $Eu_2(BA)_6(dmbpy)_2$. The degradation can also be explained by the bond distances of the structure (Table 2). Eu–N distance is longer than other bond distances; theoretically, this bond is less stable and easy to be broken down, as indicated by the broken line in Fig. 4. The IR spectrum of the complex at 267°C (Fig. 2b) showed that the fingerprint region changed (compared with Fig. 2a). The SEM pictures show that the form of the complex changed from a smooth-surface cylinder to a crackled cylinder (Fig. 3).

Table 2 Main bond lengths [5] (nm)

Eu-O1 (Eu^*-$O1^*$)	2.396(2)	Eu-N(1)	2.671(3)
Eu-O2 (Eu^*-$O2^*$)	2.523(3)	Eu-N(2)	2.570(3)
Eu^*-$O3^*$ (Eu-O3)	2.375(2)	Cl-C2	1.498(5)
Eu-$O4^*$ (Eu^*-O4)	2.388(2)	C8-C9	1.501(4)
Eu-O5 (Eu^*-$O5^*$)	2.421(2)	C15-C16	1.496(4)
Eu^*-O6 (Eu-$O6^*$)	2.352(2)		
Eu-O6 (Eu^*-$O6^*$)	2.786(2)		

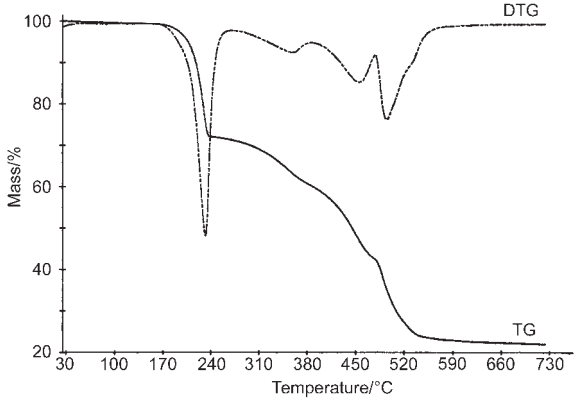

Fig. 1 TG-DTG curves of $Eu_2(BA)_6(dmbpy)_2$ using a heating rate of 5°C min^{-1} in static air; sample mass: 1.999 mg

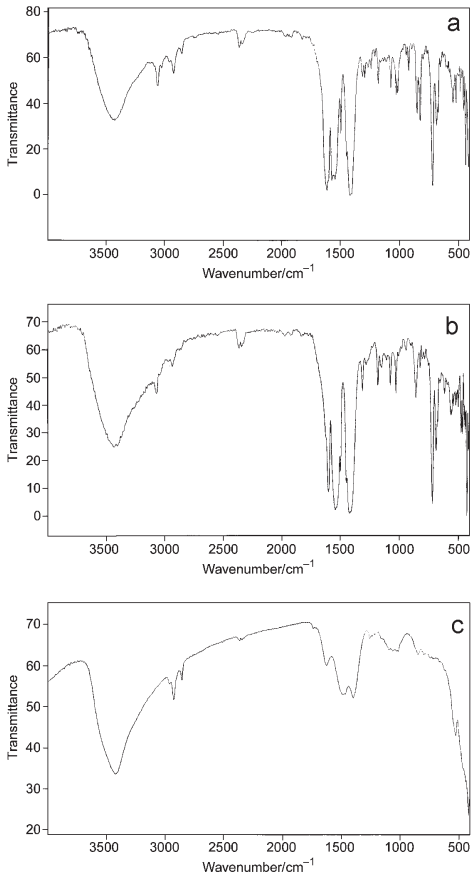

Fig. 2 IR spectra of $Eu_2(BA)_6(dmbpy)_2$; a – original complex at room temperature, b – after stage I (at 267°C), c – after stage IV (at 578°C)

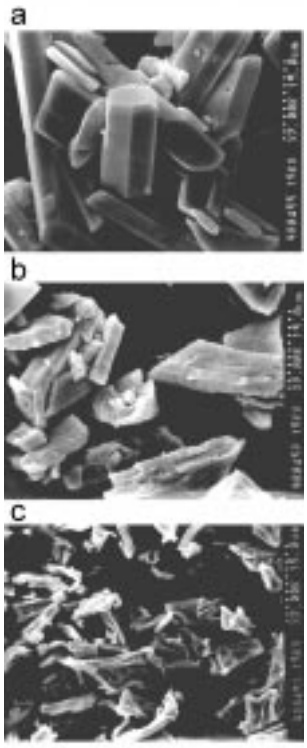

Fig. 3 Scanning electron micrographs of $Eu_2(BA)_6(dmbpy)_2$; a – original complex at room temperature; b – after stage I (at 267°C); c – after stage IV (at 578°C)

In the second stage, $Eu_2(BA)_6$ is decomposed at 267–387°C with the mass loss of 11.20%. The theoretical mass loss is 11.02% corresponding to the loss of 2 mol C_6H_5 and the formation of $Eu_2(BA)_4(COO)_2$.

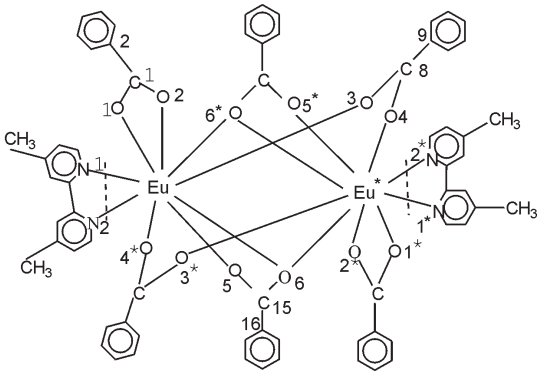

Fig. 4 Molecular structure of $Eu_2(BA)_6(dmbpy)_2$

The TG curve shows the third stage began at 387°C and completed at 479°C accompanied with 17.83% mass loss. It is in agreement with the theoretical value of the mass loss of 17.31%, corresponding to the loss of 2 mol BA and the formation of $Eu_2(BA)_2(COO)_2$.

In the fourth stage, the experimental value for the mass loss of 19.30% found between 479 and 578°C in the TG curve is in agreement with the theoretical mass loss of 20.10%, corresponding to the loss of $C_{16}H_{10}O_5$ and formation of Eu_2O_3. As shown in Fig. 2, the characteristic absorption peak for C=O group of the title complex at 1615 cm^{-1} disappeared upon heating to 578°C. The SEM pictures for the product obtained at 578°C are also completely different from that of the complex at room temperature. The formation of the above-mentioned products from (4,4'-dimethyl-2,2'-bipyridine) tris(benzoate) europium(III) should be accomplished theoretically with an overall mass loss of 74.8%, which was in agreement with the experimental value (Table 1) of 76.1%.

On the basis of experimental and calculated results, the thermal decomposition mechanism of $[Eu_2(BA)_6(dmbpy)_2]$ can be described in the following manner:

$$[Eu_2(BA)_6(dmbpy)_2] \rightarrow [Eu_2(BA)_6] \rightarrow [Eu_2(BA)_4(COO)_2] \rightarrow [Eu_2(BA)_2(COO)_2] \rightarrow Eu_2O_3$$

Non-isothermal decomposition kinetic

The basic parameters of α, T and $d\alpha/dT$ were obtained from the TG-DTG curves (Fig. 1) and summarized in Table 3. Using these parameters and 30 different mechanism function of $f(\alpha)$ and $g(\alpha)$ [8], the kinetic parameters E, $\ln A$ and linear correlation coefficients r (Table 4) were obtained with the linear least squares method. When the values of E and A obtained by the two methods are approximately equal and the linear correlation coefficient is higher, it can be concluded is characterized by the relevant function.

Table 3 Basic data for the first-stage decomposition reaction of $[Eu_2(BA)_6(dmbpy)_2]$ from TG and DTG curves

No.	T/K	α	$d\alpha/dT$	No.	T/K	α	$d\alpha/dT$
1	476.4	0.1221	0.866	12	500.5	0.6385	4.461
2	478.6	0.1405	0.978	13	502.6	0.7322	4.902
3	480.8	0.1615	1.113	14	504.8	0.8262	5.168
4	483.0	0.1863	1.283	15	505.9	0.8707	5.165
5	485.2	0.2163	1.503	16	508.1	0.9414	4.697
6	487.3	0.2513	1.774	17	510.3	0.9717	3.642
7	489.5	0.2941	2.094	18	512.5	0.9759	2.672
8	491.7	0.3997	2.467	19	514.7	0.9774	1.953
9	493.9	0.4030	2.915	20	516.9	0.9793	1.44
10	496.1	0.4721	3.417	21	519.1	0.9808	1.068
11	498.3	0.5508	3.94				

Table 4 Kinetic analysis of $[Eu_2(BA)_6(dmbpy)_2]$, stage I

Function No.	Achar method			MKN method		
	E/kJ mol^{-1}	ln$A$/s^{-1}	r	E/kJ mol^{-1}	ln$A$/s^{-1}	r
1	155.3	39.85	0.8217	215.4	49.79	0.9741
2	231.0	58.05	0.9262	250.1	57.94	0.9822
3	269.9	66.21	0.9530	267.1	60.74	0.9855
4	340.4	83.77	0.9737	303.5	69.94	0.9897
5	121.0	28.92	0.7582	191.2	41.33	0.9706
6	552.0	136.43	0.9777	444.6	105.39	0.9879
7	255.2	65.59	0.9683	179.4	42.29	0.9908
8	192.8	50.15	0.9578	117.0	26.85	0.9903
9	161.5	42.34	0.9485	85.7	19.05	0.9899
10	130.3	34.42	0.9336	54.5	11.12	0.9889
11	114.7	30.37	0.9222	38.9	7.04	0.9878
12	149.4	38.57	0.9279	134.6	30.16	0.9863
13	184.7	46.94	0.9536	147.8	33.14	0.9891
14	43.6	12.93	0.4648	103.7	22.90	0.9722
15	–12.2	–0.87	0.1692	47.9	9.07	0.9670
16	–30.8	–5.65	0.4180	29.3	4.25	0.9609
17	–40.1	–8.12	0.5256	20.0	1.70	0.9532
18	466.8	118.25	0.9613	315.3	76.58	0.9726
19	361.0	91.23	0.9668	97.8	22.95	0.9091
20	6.4	3.78	0.0853	66.5	13.74	0.9699
21	442.6	111.40	0.9800	366.8	88.06	0.9912
22	629.9	156.92	0.9840	554.1	133.56	0.9913
23	817.3	202.32	0.9860	741.5	178.94	0.9914
24	678.3	171.61	0.9520	415.2	103.26	0.9177
25	202.3	51.04	0.9602	155.0	34.69	0.9900
26	–167.9	–39.04	0.7236	67.1	13.97	0.9328
27	–379.5	–91.29	0.8391	46.6	8.82	0.8911
28	–591.0	–143.66	0.8706	33.5	5.42	0.8471
29	106.8	28.18	0.9127	69.9	14.37	0.9876
30	121.5	31.32	0.9116	63.3	12.84	0.9845

For the first stage of decomposition of the title compound, it can be suggested that the function of the possible mechanism is function No. 3, i.e. ($f(\alpha)=3/2[(1-\alpha)^{-1/3}-1]^{-1}$, $g(\alpha)=(1-2\alpha/3)-(1-\alpha)^{2/3}$) [8]. So the first stage of decomposition reaction was governed

by three-dimensional (cylindrical symmetry, Ginstling–Brounshtein equation). The activation energy of the first stage is 267–269 kJ mol^{-1}.

References

1 Y. Zhang, L. P. Jin and S. Z. Lü, J. Inorg. Chem., (in Chinese), 13 (1997) 280.
2 L. P. Jin, R. F. Wang and L. S. Li, Polyhedron, 18 (1998) 487.
3 J. J. Zhang, R. F. Wang and J. B. Li, J. Therm. Anal. Cal., 62 (2000) 747.
4 J. J. Zhang, R. F. Wang and X. L. Zhai, Chinese J. Inorg. Chem., 16 (2000) 103.
5 R. F. Wang, L. P. Jin and L. S. Li, J. Coord. Chem., 47 (1999) 279.
6 B. N. Achar, Proc. Int. Clay Conf. Jerusalem, 1 (1964) 67.
7 P. M. Madhusudhanan, K. Krishnan and K. N. Ninan, Thermochim. Acta, 7 (1986) 189.
8 J. J. Zhang, L. G. Ge and X. L. Zhang, J. Therm. Anal., Cal., 58 (1999) 269.